British Journal of Pharmacology (1995) 116, 3099-3109

Nitric oxide synthase in human placenta and umbilical cord from normal, intrauterine growth-retarded and pre-eclamptic pregnancies

*Richard A.D. Rutherford, †Andrew McCarthy, †Mark H.F. Sullivan, †Murdoch G. Elder, *Julia M. Polak & *[1]John Wharton

Departments of *Histochemistry and †Obstetrics and Gynaecology, Royal Postgraduate Medical School, Hammersmith Hospital, London W12 0NN

1 It has been suggested that a deficiency of nitric oxide (NO) may explain many of the pathophysiological features of pre-eclampsia (PE) and intra-uterine (foetal) growth retardation (IUGR). To elucidate further the role of NO in the pathophysiology of pregnancy we have determined the relative amount and activity of NO synthase (NOS) in first trimester and normal-term placental tissues, as well as in the placenta and umbilical cord in pregnancies complicated by PE and IUGR, using N^G-nitro-L-[2,3,4,5-^{3}H]-arginine ([^{3}H]-L-NOARG) binding, quantitative *in vitro* autoradiography, [^{3}H]-arginine to [^{3}H]-citrulline conversion and Western blotting.

2 Specific, high affinity ($K_D = 38$ nM) [^{3}H]-L-NOARG binding was demonstrated in the villous trophoblast of normal-term placentae. Binding was calcium-independent, stereoselective and exhibited a rank order of inhibition by NOS inhibitors and substrate (L-NOARG $\geqslant$ L-NMMA $\geqslant$ 7-NI > L-NAME > L-Arg $\geqslant$ L-NIO > ADMA).

3 [^{3}H]-L-NOARG binding density and NOS activity were both significantly greater in placental tissues from first trimester and PE or IUGR complicated pregnancies compared to normal-term placentae.

4 Western blotting, using an endothelial NOS peptide antiserum, demonstrated a ~140 KDa protein band in placental extracts and indicated that the amount of immunoreactive material was significantly greater in first trimester compared to normal-term placentae.

5 Specific [^{3}H]-L-NOARG binding was also localized to the endothelial lining of umbilical arteries and veins, binding density being greater in the artery than the vein. [^{3}H]-L-NOARG binding to the umbilical artery endothelium was significantly lower in PE and IUGR complicated pregnancies compared to normal-term controls.

6 The role of trophoblast-derived NO in human placental pathophysiology remains to be established, but differences in the amount of placental [^{3}H]-L-NOARG binding, NOS activity and immunoreactive material indicate that expression of NOS in the villous trophoblast falls during pregnancy. Conversely, the apparent reduction in NOS in the umbilical artery endothelium in PE and IUGR complicated pregnancies may be indicative of endothelial dysfunction.

Keywords: Nitric oxide synthase; quantitative autoradiography; placenta; villous trophoblast; umbilical blood vessels; endothelium; pre-eclampsia

Introduction

The human foetoplacental circulation is characterized by a low vascular resistance and unlike other vascular beds, lacks autonomic innervation (Reilly & Russell, 1977; Fox & Khong, 1990). Circulating and locally released vasoactive factors, such as the potent vasodilator and inhibitor of platelet aggregation nitric oxide (NO), are therefore likely to be important in the control of foetoplacental haemodynamics, ensuring adequate placental blood flow, foetal nutrition and oxygenation (Boura *et al.*, 1994). The release of NO has been demonstrated from human umbilical vein endothelium and exogenous NO shown to relax umbilical and chorionic plate artery preparations *in vitro* (Chaudhuri *et al.*, 1991; Hull *et al.*, 1994). NO attenuates the actions of vasoconstrictors in the foetoplacental circulation and inhibition either of NO synthesis, or of its action on vascular smooth muscle, increases basal perfusion pressure in the isolated human placental cotyledon (Gude *et al.*, 1990; 1992; Myatt *et al.*, 1991; 1992). NO has also been implicated in the pathophysiology of pregnancy, there being evidence of endothelial dysfunction and imparied maternal NO production in pregnancies complicated by pre-eclampsia (PE) (Roberts & Redman 1993; McCarthy *et al.*, 1993; Seligman *et al.*, 1994). In addition, raised plasma concentrations of the endogenous NO synthase (NOS) inhibitor N^G,N^G-asymmetric dimethylarginine (ADMA) have been found in women with PE compared to normotensive pregnant controls (Fickling *et al.*, 1993), and infusion of pregnant rats with NOS inhibitors has been shown to produce features characteristic of PE, including a loss of the pregnancy-induced refractoriness to vasoconstrictors, hypertension, proteinuria and intrauterine (foetal) growth retardation (IUGR) (Molnár & Hertelendy, 1992; Yallampalli & Garfield, 1993; Molnár *et al.*, 1994). Increased vascular resistance in the foetoplacental circulation, as indicated by abnormal umbilical artery flow velocity waveforms, is also a characteristic of PE and IUGR pregnancies (Trudinger *et al.*, 1985; Erskine & Ritchie, 1985) and, although there is evidence of diminished NO release in the umbilical artery of PE patients (Pinto *et al.*, 1991; Akar *et al.*, 1994), it is uncertain whether placental NO production is affected (Brennecke *et al.*, 1994; Kovács *et al.*, 1994; Wang *et al.*, 1994). Furthermore, the production of NO and sensitivity to NO in segments of umbilical artery has been reported to decline with increasing gestational age (Izumi *et al.*, 1994) but it is not known if there are corresponding differences in placental NOS expression and activity.

[1] Author for correspondence.

NO is generated from the conversion of L-arginine to L-citrulline by NO synthase, a reaction which requires tetrahydrobiopterin, haem, flavin adenine dinucleotide and flavin mononucleotide as cofactors, and NADPH and molecular O_2 co-substrates for enzymatic activity (see Knowles & Moncada 1994; Sessa 1994). Three main NOS isoforms have been identified and cloned, comprising neuronal (Bredt *et al.*, 1991), endothelial (Marsden *et al.*, 1992) and inducible isoforms (Xie *et al.*, 1992). These distinct enzymes display ~50% amino acid sequence homology and may be distinguished both by their subcellular localization and dependence on calcium. Endothelial NOS (eNOS) is myristoylated and associated with the cell membrane (Pollock *et al.*, 1991; Sessa *et al.*, 1993), whereas both the neuronal and inducible enzymes are cytosolic proteins (Busse & Mulsch 1990a; Stuehr *et al.*, 1991). The activity of the endothelial and neuronal isoforms is also calcium-dependent, whereas the inducible enzyme binds calmodulin in the absence of raised calcium and is tonically active (Busse & Mulsch, 1990b; Bredt & Snyder, 1990; Cho *et al.*, 1992).

Maternal NO production and eNOS expression appear to be increased during pregnancy (Conrad *et al.*, 1993a; Goetz *et al.*, 1994) and human placental tissues have been shown to express selectively the eNOS isoform (Conrad *et al.*, 1993b; Myatt *et al.*, 1993b; Garvey *et al.*, 1994). Most studies hitherto have used immunohistochemical or histochemical techniques to examine the distribution of NOS in the normal umbilical cord and placenta (Springall *et al.*, 1992; Myatt *et al.*, 1993a; Buttery *et al.*, 1994b), however, these methods are only semi-quantitative and demonstration of NADPH-diaphorase activity is not specific for NOS. *In situ* hybridization has also been employed to identify eNOS mRNA in placental sections (Conrad *et al.*, 1993b), but due to the need to measure, as well as localize, NOS in tissues from normal, PE and IUGR complicated pregnancies, we have sought an alternative quantitative method. A ^{3}H-labelled analogue of L-arginine, N^G-[2,3,4,5-^{3}H]-nitro-L-arginine ([^{3}H]-L-NOARG), has been used to characterize NOS isoforms in rat brain homogenates and tissue sections (Michel *et al.*, 1993; Kidd *et al.*, 1995). We have employed this selective inhibitor of NOS in quantitative *in vitro* autoradiographic studies, the aims of which were to determine both the localization and relative level of NOS expression in placental tissues during normal, pre-eclamptic and intrauterine (foetal) growth retarded pregnancies, and to compare the results with those obtained from measuring enzyme activity and immunoreactivity in extracts of the same placental tissues.

Methods

Tissues

Placentae were collected following elective caesarean section from normal-term pregnancies ($n=10$) and from pregnancies complicated either by pre-eclampsia (PE, $n=4$) or intrauterine foetal growth retardation without PE (IUGR, $n=13$) (Table 1). Placentae were also obtained from pregnancies complicated by both PE and IUGR ($n=17$) and delivered by elective caesarean section (Table 1). Pre-eclamptic pregnancies were characterized by proteinurea (at least 0.5 g 24 h^{-1}), a sustained rise ($\geq$30 mmHg) in the maternal diastolic blood pressure from the onset of pregnancy, and the absence of pre-existing hypertension. Intrauterine foetal growth retardation was characterized by a birth weight below the fifth centile for gestational age and in 10 of the cases examined an abnormal umbilical artery flow velocity waveform had been recorded before delivery by doppler ultrasound. A further group of normal-term placentae ($n=4$) was collected following spontaneous vaginal delivery (Table 1). Samples of first trimester villous tissue (7–12 weeks gestational age, $n=13$) were obtained following legal abortion by uterine evacuation. Tissue blocks were taken from both foetal and maternal surfaces of the placenta to include the chorionic plate, placental villi, basal plate (decidua) and umbilical cord. Placental bed biopsies were also obtained from some of the patients included in this study. In addition, placental villous tissue was snap frozen and stored in liquid nitrogen for subsequent determination of nitric oxide synthase activity. All tissues were obtained following the ethical standards of the institution in which they were collected.

Further tissues were collected from adult male Wistar rats as control samples for the detection of inducible, as well as endothelial, isoforms of nitric oxide synthase. These comprised samples of heart, lung, liver and spleen, obtained 6 h after intraperitoneal injection of either LPS from *Klebsiella pneumoniae* (20 mg kg^{-1}) or vehicle alone, as previously described (Buttery *et al.*, 1994a). Human and rat tissues were placed on cork mats, surrounded by mounting medium (Tissue-Tek, Miles Inc., Elkhart, Indiana, U.S.A.) and frozen in melting dichlorodifluoromethane (Arcton'12, ICI, Cheshire) without prior fixation. Specimens were stored either in liquid nitrogen or at −40°C.

In vitro *autoradiography*

Cryostat sections (10 μm thick) were thaw-mounted onto chrom-alum gelatin coated glass slides, dried and used immediately or stored at −20°C with silica gel until use. Pilot studies demonstrated that storage of specimens, either as frozen blocks or sections on slides, had no detectable effect on [^{3}H]-L-NOARG binding. Sections were pre-incubated in 50 mM Tris-HCl buffer (pH 7.3) for 15 min and then in fresh buffer containing 10 μM $CaCl_2$ and 5–200 nM [^{3}H]-L-NOARG, for up to 30 min. Incubations were performed in humid chambers at 20°C. Following incubation, the slides were washed twice in buffer at 4°C for 5 min, rinsed in distilled water at 4°C and dried under a stream of cold air. Autoradiographic images were produced by exposing dry, labelled

Table 1 Clinical features of pregnancies

Pregnancies	*Birth weight* (kg)	*Gestational age* (weeks)	*Maternal age* (years)	*Systolic blood pressure* (mmHg)	*Diastolic blood pressure* (mmHg)
Normal term					
Caesarian ($n=10$)	3.5 (3.1–3.9)	39 (38–40)	28 (24–32)	119 (109–129)	74 (67–82)
Transvaginal ($n=4$)	3.5 (3.0–4.1)	40 (39–41)	29 (21–37)	124 (116–131)	78 (70–85)
Pre-eclampsia ($n=4$)	2.3 (1.8–2.8)**	35 (31–39)*	23 (16–30)	151 (137–165)*	106 (94–118)**
PE/IUGR ($n=17$)	1.1 (0.9–1.3)**	30 (29–32)**	30 (28–32)	152 (145–160)*	106 (103–110)**
IUGR ($n=11$)	1.3 (0.9–1.8)**	32 (30–34)**	33 (30–36)	126 (110–143)	80 (71–90)
1st Trimester ($n=13$)	–	10 (7–13)**	–	–	–

Values are expressed as the mean and 95% confidence interval (95% CI). Significant difference (*$P<0.01$ and **$P<0.001$) in pregnancies complicated by pre-eclampsia (PE), pre-eclampsia and intrauterine foetal growth retardation (PE/IUGR) and intrauterine foetal growth retardation (IUGR) compared with normal-term and first trimester placentae.

sections to Hyperfilm-^{3}H for up to 6 weeks at 4°C, developed in Kodak D-19 developer for 4–5 min, fixed in Amfix and rinsed in running water. Further anatomical resolution of binding sites was achieved by microautoradiography, labelled sections being exposed to emulsion-coated coverslips for 8 weeks at 4°C.

Quantification and characterization of NOS binding

[^{3}H]-L-NOARG binding to placental tissue sections was quantified either by scintillation counting or autoradiography. Binding to other tissues was determined by autoradiography alone. For scintillation counting, labelled sections were removed from slides into scintillation vials, by use of a piece of filter paper, 2 ml of scintillation fluid (Ready Gel, Beckman Instruments Inc., Fullerton, Ca. U.S.A.) was added and the radioactivity measured in a scintillation counter (Beckman Model LS6800). Each sample was counted for 5 min and the results converted to disintegrations per min (d.p.m.) following correction for the efficiency of the counter. An IBAS 386 Image Analysis System (Kontron Elektronic, Watford, U.K.) was used to quantify [^{3}H]-L-NOARG binding to specific tissue structures in autoradiographic film images. Standard curves relating grey values to log concentration of [^{3}H]-L-NOARG bound (amol mm^{-2}) were obtained for each film by autoradiographic ^{3}H-microscale standards. Non-specific binding was defined as that remaining in the presence of an excess (10^{-5} M) of unlabelled ligand, L-NAME or L-NMMA. Specific binding was determined by subtracting the non-specific binding from the total binding in serial sections. The calcium and calmodulin sensitivity of binding was assessed by the addition of either EGTA (1 mM), calcium chloride (0.001–1.0 mM), A23187 (1 μM), calmodulin (100–500 u ml^{-1}), the calmodulin antagonists fluphenazine N-mustard dihydrochloride and trifluoperazine (100 μM) or the phosphodiesterase inhibitor IBMX (1 mM) to the pre-incubation and/or incubation buffers. The effect of the co-factor NADPH on binding was assessed by conducting binding experiments in the presence of 0–10 mM NADPH.

Association binding kinetics were examined by incubating serial sections of placentae with 10 nM [^{3}H]-L-NOARG for 1–30 min at 20°C. Dissociation kinetics were determined following the addition of 10 μM unlabelled L-NOARG to sections after 15 min incubation and incubating for a further 90 min. The kinetic constants for association (k_{+1}) and dissociation (k_{-1}), and the equilibrium dissociation constant (K_D) were derived from kinetic binding data. Saturation studies were also performed by incubating adjacent sections with increasing concentrations of [^{3}H]-L-NOARG (0.5–200 nM), alone and in the presence of 10 μM unlabelled L-NOARG. Competitive inhibition experiments were used to investigate the specificity of [^{3}H]-L-NOARG binding, sections being incubated in the presence of increasing concentrations (10^{-13}–10^{-5} M) of unlabelled substrate, stereoisomers or NOS inhibitors. The possibility of ligand binding to an amino acid uptake or transporter system was investigated by incubating sections with [^{3}H]-L-NOARG in the presence of increasing concentrations (10^{-5} to 10^{-2} M) of either L-leucine, L-isoleucine, L-ornithine or L-lysine. Binding data were analyzed by iterative non-linear regression by GraphPad InPlot version 4.03 (GraphPad Software, San Diego, U.S.A.). A four parameter logistic equation was used to describe the relationship between [^{3}H]-L-NOARG bound and the concentration of NOS substrate or inhibitor in competitive inhibition experiments. Data from inhibition experiments were fitted to one or two site models and the 'best fit' sums of squares compared statistically by an F-test. The concentration of unlabelled ligand which produced 50% inhibition of specific [^{3}H]-L-NOARG binding (IC_{50} value) was calculated from binding inhibition experiments and the inhibition constant (K_i) derived according to the equation of Cheng & Prusoff (1973), $K_i = IC_{50}/1 + [L]/K_D$), where [L] is the ligand concentration and K_D the equilibrium dissociation constant derived from saturation analysis.

Nitric oxide synthase activity

Extracts of placentae were assayed for enzyme activity by measuring the conversion of [^{3}H]-arginine to [^{3}H]-citrulline, essentially as previously described and validated by thin-layer chromatography (Conrad *et al.*, 1993b). Briefly, 0.35–0.75 g of placental tissue, initially frozen in liquid nitrogen, was homogenized in 10 volumes of 25 mM HEPES buffer (pH 7.4) containing 50 mM sucrose, 1 mM DTT and 10 mg ml^{-1} each of the protease inhibitors leupeptin, pepstatin A, chymostatin, bestatin and soybean trypsin inhibitor as well as 100 mg ml^{-1} of phenylmethylsulphonyl fluoride. The homogenate was then centrifuged for 15 min at 1000 g and the supernatant passed over 10DG columns and the eluate (100 μl) added to an equal volume of incubation buffer whose final concentration of co-factors and substrates was: calmodulin (10 u ml^{-1}), FAD (10 μM), NADPH (0.5 mM), BH_4 (2 μM), L-valine (50 mM), $CaCl_2$ (10 μM), L-arginine (2 μM) and [^{3}H]-L-Arg (5 μCi ml^{-1}). The calcium dependency of the reaction was assessed by incubation in the presence of EGTA (0.5 mM) and the effect of inhibition of NOS on the production of [^{3}H]-L-citrulline was determined by the inclusion of the specific inhibitor, L-NAME (0.1 mM). The incubations were performed at 30°C in a shaking water bath for 40 min and stopped by adding 1.3 ml of ice-cold 80 mM HEPES buffer (pH 5.2) containing 8 mM EDTA. The [^{3}H]-L-citrulline produced in the reaction was separated from [^{3}H]-L-arginine by Dowex AG50W-x8 cation exchange columns (Na^+ form), >95% of the counts being eluted in the first 3 ml of eluate. Protein was measured by use of the Bio-Rad protein reagent with BSA as standard.

Western blotting

Placental homogenate fractions were standardised for protein content (20 μg/sample) and separated by 7.5% sodium-dodecyl-sulphate polyacrylamide gel electrophoresis (SDS-PAGE) according to Laemmli (1970). The samples were then blotted in 20% methanol, Tris (25 mM), glycine (192 mM) onto nitrocellulose membranes (Schleicher & Schuell, Dassel, Germany) and blocked overnight at 4°C with 3% non-fat dry milk in PBS-Tween buffer (50 mM PBS, pH 7.4 and 0.1% Tween). After washing (4 × 5 min each), the blots were incubated with a monoclonal antibody to eNOS (H32, diluted 1 : 5000 in PBS, 0.1% BSA) for 1 h at room temperature, washed (4 × 5 min each) and then incubated with horseradish peroxidase-conjugated goat anti-mouse IgG (diluted 1 : 1000) for 45 min at room temperature. Blots were then rinsed (4 × 5 min each) and the specific proteins detected by enhanced chemiluminescence (ECL, Amersham). The integrated optical density for each sample was determined by quantitative analysis of the ECL-autoradiographic film by a Seescan 'Symphony' image analysis system (Seescan plc., Cambridge, U.K.).

Immunohistochemistry

To confirm ligand binding to endothelial and villous trophoblast cells, labelled sections were immunostained for CD31 and cytokeratin respectively by specific monoclonal antisera and indirect immunofluorescence staining. Sections were fixed for 10 min in acetone at 4°C, incubated with primary antisera overnight at 4°C, incubated with fluorescein isothiocyanate-labelled goat anti-mouse IgG (1 : 100) for 1 h at room temperature, and examined by an Olympus AH2 fluorescence microscope. Controls included the omission of the primary antiserum and replacement with non-immune serum.

Reagents

N^G - nitro - L - [2,3,4,5 - ^{3}H - arginine hydrochloride ([^{3}H] - L - NOARG), L-[2,3,4,5-^{3}H]-arginine hydrochloride ([^{3}H]-L-Arg), Hyperfilm-^{3}H and autoradiographic [^{3}H]-microscales were obtained from Amersham International (Amersham, U.K.). L-Arginine (L-Arg); D-arginine (D-Arg); L-leucine; L-isoleucine;

L-ornithine; L-lysine; L-valine; N^G-nitro-L-arginine (L-NOARG); N-iminoethyl-L-ornithine (L-NIO); N^G-nitro-arginine methyl ester (L-NAME); N^G-monomethyl-L-arginine(L-NMMA); asymmetric N^G,N^G,-dimethylarginine (ADMA); symmetric N^G,$N^{G'}$-dimethylarginine; aminoguanidine; flavin adenine dinucleotide (FAD) and protease inhibitors were obtained from Sigma Chemical Company, Poole, U.K. 7-Nitroindazole (7-NI) was purchased from Cookson Chemicals, Southampton, U.K. Fluphenazine N-mustard dihydrochloride was from Research Biochemicals Inc., Natick, MA, U.S.A. Calmodulin, trifluoperazine dihydrochloride, 3-isobutyl-1-methylxanthine (IBMX), A23187, nicotinamide adenine dinucleotide phosphate (NADPH) and lipopolysaccharide (LPS) from *Klebsiella pneumoniae* were from Sigma. Antiserum to CD31 (platelet cell adhesion molecule; code JC/70A) was obtained from Dako Ltd., High Wycombe, U.K. Antiserum to cytokeratin (peptide 18), fluorescein isothiocyanate-labelled goat anti-mouse IgG and horseradish peroxidase-conjugated goat anti-mouse IgG were from Sigma. A monoclonal antibody (H32) against bovine aortic eNOS was provided by Dr J. Pollock (Abbott Laboratories, Chicago, IL., USA) (Pollock *et al.*, 1993). 10DG columns, Dowex AG50W-x8 cation exchange columns (Na^+ form) and protein assay reagent were obtained from Bio-Rad Laboratories Ltd., Hemel Hempstead, U.K.

Statistics

Values are expressed as arithmetic or geometric means as appropriate with 95% confidence intervals (95% CI). Binding data were analysed by Student's *t* test, analysis of variance or nonparametric methods, as appropriate, differences being considered significant if the *P* value was less than 0.05. To reduce the probability of significant differences arising by chance, Bonferroni's correction was applied to the data following analysis of variance (Wallenstein *et al.*, 1980).

Results

Specific [^{3}H]-L-NOARG binding was localized to the villous trophoblast in both first trimester and normal-term placentae, as well as to the endothelium of the umbilical blood vessels, in all the samples examined. Relatively high density, homogeneous binding was observed throughout the villous trophoblast (Figure 1) and to the endothelial lining of both the umbilical vein and arteries (Figure 2). Binding was also localized to trophoblast cells invading spiral arteries in the placental bed. Vascular binding sites exhibited a differential distribution pattern, the density of binding in normal-term umbilical arteries (5242 amol mm^{-2}; 4319–6166 95% CI; $n=15$) being significantly greater ($P=0.0262$) than that demonstrated in umbilical veins (4329; 3962–4966 95% CI; $n=15$). The density of binding declined in more distal regions of the placental vasculature, [^{3}H]-L-NOARG binding localized to the endothelium of vessels in the chorionic plate and stem villi (1032 amol mm^{-2}, 861–1204 95% CI; $n=9$) being significantly less ($P<0.01$) than that demonstrated in umbilical blood vessels. In distal regions of the villous tree, [^{3}H]-L-NOARG binding was mainly localized to the villous trophoblast, relatively little binding being demonstrated to the vascular endothelium (Figure 3). The cellular localization of [^{3}H]-L-NOARG binding was confirmed immunohistochemically, villous trophoblast cells showing cytokeratin immunoreactivity (Figure 4) and vascular endothelial cells displaying immunofluorescence staining for the glycoprotein CD31 (Figure 5). No specific binding was demonstrated to decidual cells, extravillous trophoblast cells or vascular smooth muscle and nonspecific binding represented 7–19% of total binding.

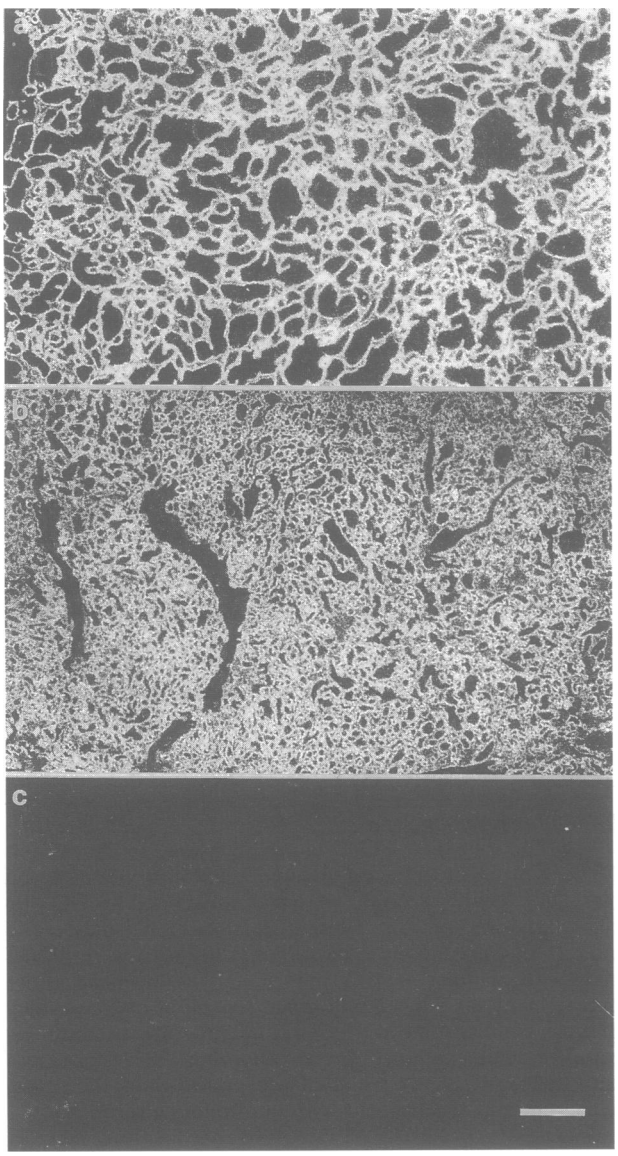

Figure 1 Reversal prints of film autoradiograms demonstrating the localization of [^{3}H]-L-NOARG binding to sections of villous tissue in the first trimester (a) and normal-term human placenta (b, c), in the absence (a, b) and presence (c) of 10^{-5} M unlabelled L-NOARG. Binding is localized to the villous trophoblast throughout the placenta and is completely inhibited in the presence of an excess of unlabelled ligand. Bar = 1 mm.

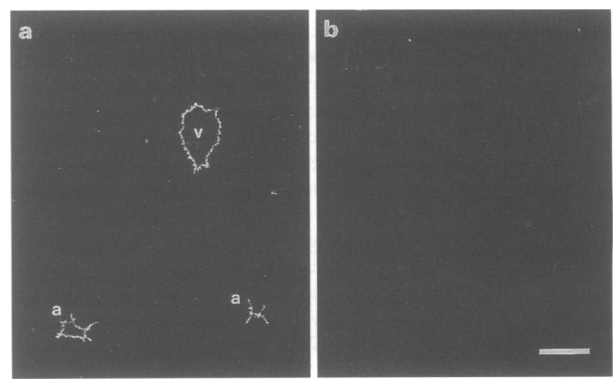

Figure 2 Reversal prints of film autoradiograms showing the localization of [^{3}H]-L-NOARG binding to serial sections of normal-term umbilical cord (a, b), in the absence (a) and presence of 10^{-5} M unlabelled L-NOARG (b). Binding is localized to the endothelial lining of the umbilical vein (v) and arteries (a) and is completely inhibited in the presence of an excess of unlabelled ligand. Bar = 1 mm.

Possible binding of [^{3}H]-L-NOARG to amino acid transporter systems was investigated by incubating sections in the presence of an increasing concentration (10^{-5} to 10^{-2} M) of either L-leucine, L-isoleucine, L-ornithine or L-lysine, however, none of these amino acids had a significant effect on equilibrium binding. [^{3}H]-L-NOARG binding was apparently calcium- and calmodulin-independent, being unaffected by the presence of either EGTA, calcium chloride, A23187, calmodulin, fluphenazine N-mustard, trifluoperazine or IBMX. The presence of 0–10 mM NADPH in the incubation buffers also had no detectable effect on ligand binding. No difference was detected in either the distribution or density of [^{3}H]-L-NOARG binding in sections of rat heart, lung, liver or spleen obtained 6 h after the induction of NOS by LPS injection, compared to that seen in tissues from control animals (data not shown).

Association binding experiments indicated that the binding of [^{3}H]-L-NOARG (10 nM) to human placenta was time-dependent and reached an apparent equilibrium by 15 min at 20°C (Figure 6). Dissociation of the ligand, following the addition of 10 μM unlabelled L-NOARG, was rapid with only 30% remaining after 30 min (Figure 6). Analysis of association and dissociation binding data gave association (k_{+1}) and dissociation (k_{-1}) rate constants of 8.6×10^4 M^{-1} s^{-1} (2.3×10^4–14.8×10^4, 95% CI) and 18.3×10^{-4} M^{-1} s^{-1} (3.3×10^{-4}–26.7×10^{-4}, 95% CI) respectively and an equilibrium dissociation rate constant (K_D) of 47.7 nM (8.1–87.4, 95% CI). Binding to human placenta was saturable and of high affinity, the K_D value (38.1 nM; 27.4–48.9, 95% CI) derived from non-linear regression analysis of saturation binding data (Figure 7) being similar to that obtained from kinetic binding studies.

Competitive inhibition of specific [^{3}H]-L-NOARG binding by unlabelled NOS inhibitors and substrate demonstrated significant differences in inhibitory potency, with a rank order of L-NOARG $\geq$ L-NMMA $\geq$ 7-NI > L-NAME > L-Arg $\geq$ L-NIO > ADMA and binding curves were best fitted to a single site model (Figure 8; Table 2). In contrast to other inhibitors used, placental binding was not inhibited by the selective inhibitor of inducible NOS, aminoguanidine (not shown). [^{3}H]-L-NOARG binding was completely inhibited by the enzyme substrate L-Arg whereas D-Arg showed no inhibitory potency (Figure 8). Similarly, the endogenous NOS inhibitor ADMA inhibited [^{3}H]-L-NOARG binding (Table 2) whereas the inactive symmetric isomer of dimethylarginine had no significant inhibitory effect (not shown).

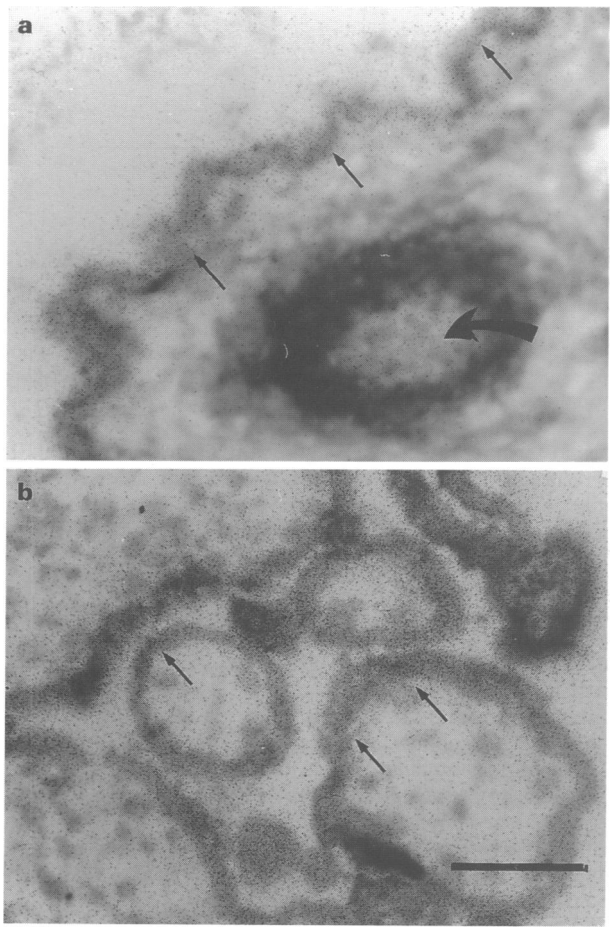

Figure 3 Brightfield photomicrographs of normal-term placental villi showing the microscopic localization of [^{3}H]-L-NOARG binding to the villous trophoblast (small arrows). Endothelial cells in villous arterioles (large arrow) exhibit relatively low density binding (a) and no endothelial binding is demonstrated in more distal regions of the villous tree (b). Bar = 100 μm.

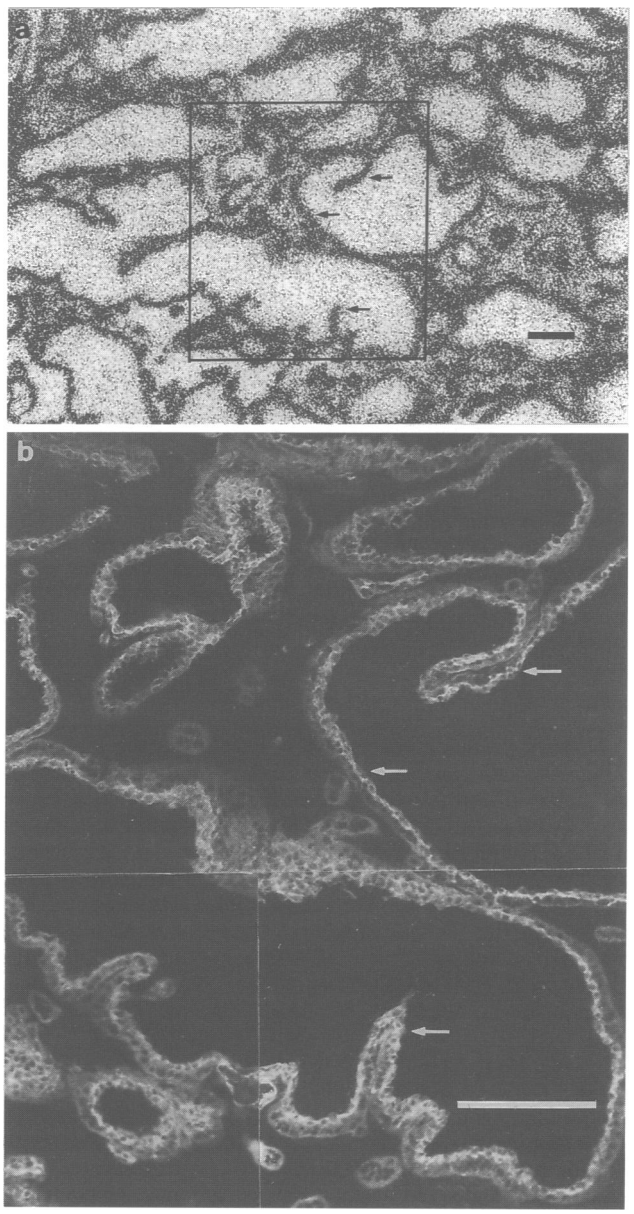

Figure 4 Photomicrographs of a section of first trimester villous tissue demonstrating the colocalization (arrows) of [^{3}H]-L-NOARG binding (a) and cytokeratin immunoreactivity (b) to the villous trophoblast. Square in (a) corresponds to the area in the same section showing cytokeratin immunoreactivity (b). The syncytiotrophoblast exhibits more intense immunofluorescence staining than the underlying cytotrophoblast. Bar = 200 μm.

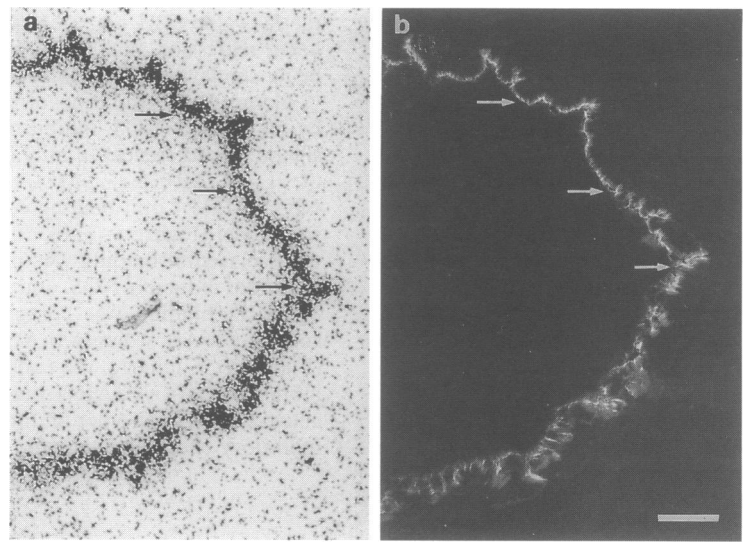

Figure 5 Photomicrographs of a section of umbilical vein demonstrating the colocalization (arrows) of [^{3}H]-L-NOARG binding to the endothelium (a), which displays immunofluorescence staining for the glycoprotein CD31 (b). Bar = 100 μm.

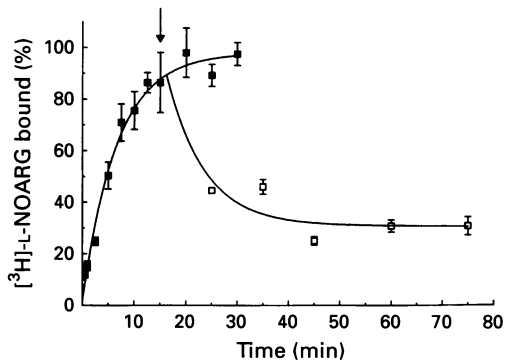

Figure 6 Association (■) and dissociation (□) of 10 nM [^{3}H]-L-NOARG to sections of human placenta at 20°C. At apparent equilibrium the incubation buffer was removed and replaced by buffer containing an excess (10^{-5} M) of unlabelled L-NOARG (arrow). Each point represents the mean ± s.e.mean specific binding for six separate normal-term placentae.

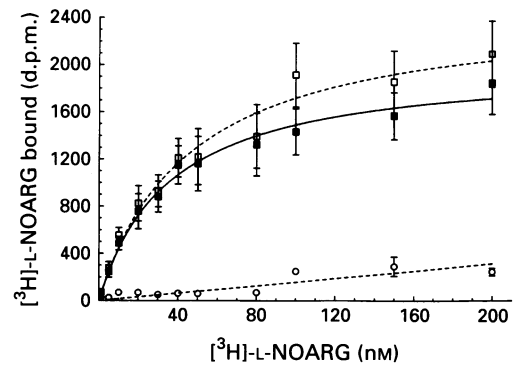

Figure 7 Saturation analysis of specific [^{3}H]-L-NOARG binding (■) to sections of human placenta. Sections were incubated with increasing concentrations (0.5–200 nM) of [^{3}H]-L-NOARG in the absence (total binding, □) and presence (non-specific binding, ○) of 10^{-5} M unlabelled L-NOARG at 20°C for 15 min. Each point represents the mean ± s.e.mean specific binding for six separate normal-term placentae.

No significant differences were detected in the binding to either the villous trophoblast or umbilical vascular endothelium in normal-term placentae delivered by elective caesarean section or transvaginal delivery. A similar distribution of [^{3}H]-L-NOARG binding sites was observed in the placentae and umbilical cords from normal and complicated pregnancies. However, quantitative analysis of autoradiograms demonstrated that significantly more ligand was bound to the villous trophoblast in the first trimester (13,570 amol mm^{-2}; 10811–16329 95% CI; $n=4$; $P<0.001$) and in placentae from pregnancies complicated by either PE (6771 amol mm^{-2}; 5680–7862 95% CI; $n=4$; $P=0.005$), PE/IUGR (6460 amol mm^{-2}; 5551–7370 95% CI; $n=17$; $P=0.0009$) or IUGR (5957 amol mm^{-2}; 4874–7040 95% CI; $n=11$; $P=0.0121$), compared to normal-term controls (4278 amol mm^{-2}; 3433–5123 95% CI; $n=14$) (Figure 9). Placentae from PE, PE/IUGR and IUGR complicated pregnancies were delivered at an earlier gestational age compared to normal-term controls (Table 1). Linear regression analysis of the binding data indicated, however, that there was no significant correlation between [^{3}H]-L-NOARG binding density and gestational age (range 27–37 weeks) in the complicated pregnancies as a whole ($P=0.5818$), nor in the PE ($P=0.8196$), PE/IUGR ($P=0.2167$) or IUGR ($P=0.3503$) groups alone. While binding to umbilical artery endothelium in normal-term controls was significantly greater than in the corresponding veins (Table 3), no significant differences were found between endothelial binding to umbilical arteries and veins in pregnancies complicated by IUGR ($P=0.112$) and PE ($P=0.163$) (Table 3), irrespective of whether an abnormal or normal umbilical artery flow velocity waveform had been recorded during the pregnancy. Comparison of relative binding densities indicated that binding to the endothelium of umbilical arteries was significantly less in the pregnancies complicated by IUGR ($P=0.0146$) and PE ($P=0.004$) compared to controls, whereas no significant difference ($P>0.40$) was found in binding to umbilical vein endothelium (Table 3).

Placental homogenates from first trimester, PE/IUGR and normal-term pregnancies demonstrated [^{3}H]-L-Arg to [^{3}H]-L-citrulline conversion over a 40 min incubation period. Enzymatic activity was calcium-dependent, being significantly inhibited in the presence of 0.5 mM EGTA, and was almost abolished by the inclusion of 0.1 mM of the competitive NOS inhibitor, L-NAME (Figure 10). Significant differences in the level of enzyme activity, corresponding to those observed in the relative amount of [^{3}H]-L-NOARG binding, were found in placentae from first trimester, PE and IUGR complicated and normal-term pregnancies. Villous tissue from first trimester pregnancies demonstrated a 2.5 fold ($P<0.02$) and 4 fold ($P<0.01$) higher level of enzyme activity (426 pmol mg^{-1}

protein; 260–591 95% CI; $n=13$) than that observed in placentae from PE/IUGR (152 pmol mg^{-1} protein; 109–194 95% CI; $n=12$) and normal-term (100 pmol mg^{-1} protein; 72–128 95% CI; $n=10$) pregnancies respectively. A significantly higher level of enzyme activity ($P<0.05$) was also observed in placentae from PE/IUGR pregnancies compared with those from normal-term pregnancies (Figure 10).

Western blotting of the placental homogenates identified a ~140kDa band using a monoclonal antibody specific for eNOS (Figure 11). This band was not detected when the blots were incubated with pre-immune serum. Quantification of the autoradiographic images demonstrated that the integrated optical density of the immunoreactive band was significantly greater in samples of first trimester villous tissue (0.43; 0.40–

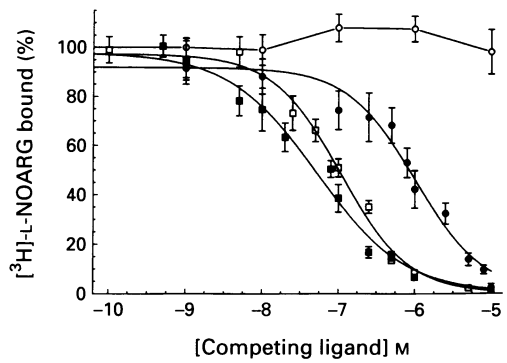

Figure 8 Competitive inhibition of specific [^{3}H]-L-NOARG binding to sections of human placenta. Serial sections were incubated with [^{3}H]-L-NOARG for 15 min at 20°C in the presence of increasing concentrations (10^{-13}–10^{-5} M) of unlabelled L-NOARG (■), L-NAME (□), L-arginine (●) and D-arginine (○). Each point represents the mean ± s.e.mean of specific binding for 5 separate normal-term placentae, expressed as a percentage of [^{3}H]-L-NOARG binding in the absence of unlabelled competitor.

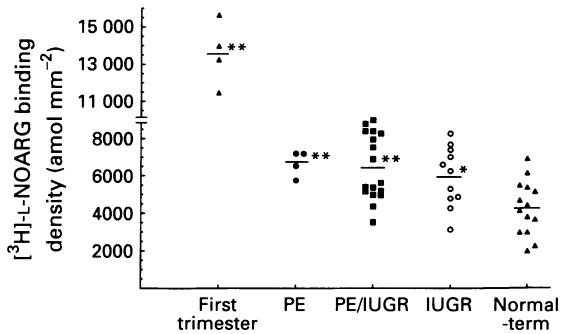

Figure 9 Relative density (amol mm^{-2}) of [^{3}H]-L-NOARG binding in sections of placenta from first trimester (△, $n=4$), pre-eclamptic (PE, ●, $n=4$), pre-eclamptic and intrauterine foetal growth retarded (PE/IUGR, ■, $n=17$), intrauterine foetal growth retarded (IUGR, ○, $n=11$) and normal-term pregnancies (▲, $n=14$). Bars represent the mean value for each group, determined by incubating sections from separate placentae with 100 nM [^{3}H]-L-NOARG for 15 min at 20°C. Binding density in first trimester, PE, PE/IUGR and IUGR complicated pregnancies is significantly greater (*$P<0.05$; **$P<0.01$) than that detected in normal-term controls.

Table 2 Competitive inhibition of [^{3}H]-L-NOARG binding to human placental sections

Competitor	K_i (nM) (95% CI)	*nH* (95% CI)
N^G-nitro-L-arginine (L-NOARG)	17.8 (8.6–33.5)	0.89 (0.46–1.32)
N^G-monomethyl-L-arginine (L-NMMA)	28.2 (23.1–34.0)	1.03 (0.85–1.22)
7-Nitroindazole (7-NI)	32.7 (19.7–48.9)	0.59 (0.42–0.76)
N^G-nitro-L-arginine methyl ester (L-NAME)	94.5* (58.9–148.2)	1.09 (0.70–1.47)
L-Arginine (L-Arg)	211.5* (37.8–646.6)	0.92 (0.52–1.32)
N-Iminoethyl-L-ornithine (L-NIO)	214.9* (137.6–319.6)	1.08 (0.80–1.36)
Asymmetric N^G,N^G-dimethylarginine (ADMA)	649.7* (323.6–1262.3)	0.73 (0.42–1.04)

K_i and Hill coefficient (nH) values derived from non-linear regression analysis of competitive inhibition data, expressed as the mean and 95% confidence interval (95% CI) for six separate placentae. *Significantly lower inhibitory potency ($P<0.05$) compared to L-NOARG.

Table 3 Relative density of [^{3}H]-L-NOARG binding to endothelium in umbilical artery and vein

	[^{3}H]-L-NOARG bound (amol mm^{-2}) *Normal-term* ($n=14$)	*IUGR* ($n=8$)	*PE/IUGR* ($n=17$)
Artery	5242 (4319–6166)	3560 (2871–4249)[a]	3627 (2959–4295)[b]
Vein	4329 (3692–4966)[c]	4377 (3562–5191)	3990 (3430–4550)

Normal-term placentae delivered by elective caesarean section and spontaneous vaginal delivery; IUGR, intrauterine foetal growth retardation alone; PE/IUGR, pre-eclamptic and intrauterine foetal growth retarded pregnancies. Specific binding of 100 nM [^{3}H]-L-NOARG for 15 min at 20°C, expressed as mean and 95% confidence interval. The mean value of binding to both arteries was obtained for each case. Significantly lower density binding to umbilical artery endothelium in IUGR ([a] $P=0.0146$) and PE/IUGR complicated pregnancies ([b] $P=0.004$), compared to normal-term controls. Density of endothelial binding in normal-term controls significantly less ([c] $P<0.05$) in umbilical vein compared to artery.

0.45 95% CI; $n=4$) than in placentae from normal-term pregnancies (0.38; 0.37–0.38 95% CI; $P=0.029$; $n=4$). Measurement of the immunoreactive band in samples from PE/IUGR complicated pregnancies (0.39; 0.37–0.41 95% CI; $n=4$) indicated that it was less than that in first trimester villous tissue ($P=0.054$) but not different from that in the normal-term samples ($P=0.2208$).

Discussion

The validity of the autoradiographic method for detecting and comparing the amount of NOS in tissue sections was shown by (1) the high affinity of [^{3}H]-L-NOARG binding and the selective inhibition of binding by other NOS inhibitors as well as by the substrate L-Arg; (2) the stereoselective inhibition of [^{3}H]-L-NOARG binding; (3) the absence of binding to an amino acid transporter system; (4) the distinct localization of binding sites in tissue sections; and (5) corresponding differences in the amount of enzyme detected by [^{3}H]-L-NOARG binding, eNOS immunoreactivity shown by Western blotting and by the level of enzyme activity demonstrated by the conversion of [^{3}H]-L-arginine to [^{3}H]-L-citrulline, in first trimester, PE, IUGR and normal-term pregnancies.

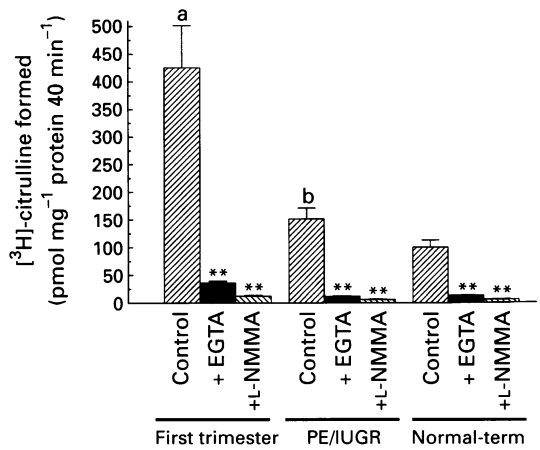

Figure 10 Production of [^{3}H]-L-citrulline from [^{3}H]-L-arginine in extracts of placental tissues from normal-term controls and pregnancies complicated by pre-eclampsia and intrauterine foetal growth retardation (PE/IUGR) and of villous tissue from first trimester pregnancies. [^{3}H]-L-citrulline production is significantly reduced (**$P<0.0001$) in the absence of calcium (+EGTA 0.5 mM) and by the addition of the NOS inhibitor L-NMMA (0.1 mM), and is significantly greater in tissues from first trimester ($^aP<0.01$) and PE/IUGR complicated pregnancies ($^bP<0.05$) compared to controls.

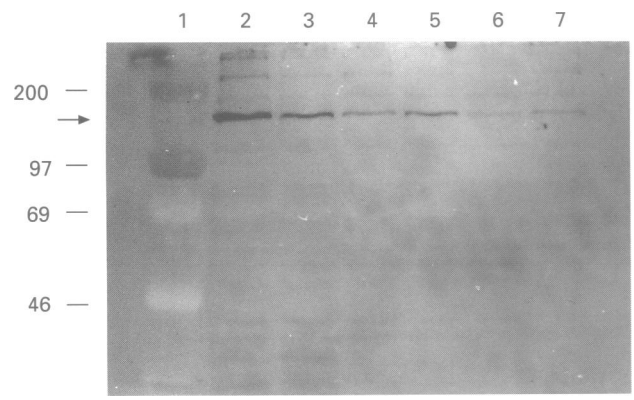

Figure 11 Western blot showing an endothelial nitric oxide synthase (eNOS)-immunoreactive band (~140 KDa) in representative extracts of first trimester villous tissue (lanes 2–3), placental tissues from pregnancies complicated by pre-eclampsia and intrauterine foetal growth retardation (PE/IUGR) (lanes 4–5) and normal-term pregnancies (lanes 6–7). Molecular weight markers (lane 1). Approximately 20 μg of protein was applied per lane.

Specific, high affinity and saturable [^{3}H]-L-NOARG binding was demonstrated in sections of human placentae from normal, PE and IUGR pregnancies, and was co-localized with cytokeratin immunoreactivity to the villous trophoblast in both first trimester and term placentae. Cytokeratin immunoreactivity was found to exhibit a distinct localization in the villous trophoblast, but due to the limited resolution of the autoradiographic technique, we were unable to establish whether there was a corresponding differential distribution of [^{3}H]-L-NOARG binding to the cytotrophoblast and syncytiotrophoblast, similar to that recently found for eNOS immunoreactivity (Eis *et al.*, 1995). In addition to the villous trophoblast, binding was localized to the endothelia of umbilical arteries and veins and to a lesser extent, blood vessels in the chorionic plate and stem villi, all of which demonstrated immunoreactivity for the endothelial marker, CD31. These findings are in accord with previous immunohistochemical (Springall *et al.*, 1992; Myatt *et al.*, 1993a; Buttery *et al.*, 1994b) and *in situ* hybridization studies (Conrad *et al.*, 1993b) demonstrating the expression of a constitutive eNOS isoform in placental tissues, localized to the villous trophoblast, and vascular endothelium in the umbilical cord and proximal rather than distal regions of the villous vascular tree.

Association, dissociation and saturation analysis of placental [^{3}H]-L-NOARG binding provided similar estimates of the equilibrium dissociation constant ($K_D \sim 38-48$nM) for binding to placental sections, and an identical estimate has been obtained by independent investigators following purification and characterization of constitutive eNOS from human placenta (Garvey *et al.*, 1994). Analysis of the monophasic inhibition curves indicated a single homogeneous population of placental binding sites and differences in the inhibitory potencies of unlabelled L-NOARG, L-Arg and the competitive NOS inhibitors L-NAME, L-NMMA, 7-NI, L-NIO and L-ADMA, as well as the stereoselectivity of binding inhibition, indicated that [^{3}H]-L-NOARG was bound to a constitutive isoform of NOS. The rank order of potency for the inhibition of placental binding corresponds with that determined for [^{3}H]-L-NOARG binding to neuronal NOS in rat brain homogenates (Michel *et al.*, 1993). L-NOARG displayed a high affinity for placental NOS and has been shown to be a selective inhibitor of constitutive NOS, exhibiting a 300 fold higher affinity for constitutive neuronal NOS than for the inducible mouse macrophage isoform of the enzyme (Furfine *et al.*, 1993). Aminoguanidine, on the other hand, is up to 100 fold more potent in inhibiting inducible NOS compared to constitutive eNOS (Hasan *et al.*, 1993; Misko *et al.*, 1993), and showed no inhibition of placental [^{3}H]-L-NOARG binding. The selectivity of [^{3}H]-L-NOARG binding for the demonstration of constitutive endothelial and neuronal NOS, rather than inducible NOS, was further underlined by the finding that there was no increase in radiolabelled inhibitor binding to rat tissues expressing inducible NOS as a consequence of LPS treatment.

Both neuronal and endothelial isoforms of NOS are considered to be dependent on intracellular calcium and calmodulin for the activity (Busse & Mulsch, 1990b; Bredt & Snyder, 1990), but it is uncertain whether the binding of L-Arg or NOS inhibitors to the enzyme also requires calcium. In the present study, [^{3}H]-L-NOARG binding was found to be insensitive to the effects of $CaCl_2$, EGTA, calmodulin and the calmodulin antagonists, fluphenazine mustard and difluoperazine. The majority of [^{3}H]-L-NOARG binding detected in rat brain homogenates has also been shown to be calcium-insensitive, although ~33% was found to be calcium-sensitive (Michel *et al.*, 1993). The reason for this apparent discrepancy is unclear

but may reflect differences in the techniques employed and tissues examined. Michel and co-workers using cytosolic preparations for their ligand binding studies. In contrast to the calcium-independent binding of [^{3}H]-L-NOARG observed in sections of placenta, the activity of the enzyme measured in placental extracts was calcium-dependent, and is consistent with the selective expression of eNOS in placental tissues (Conrad *et al.*, 1993b; Myatt *et al.*, 1993b; Garvey *et al.*, 1994).

A number of studies have proposed that endothelial cells and macrophages can take up NOS inhibitors by system y^+ and system L transporters (White, 1985; Bogle *et al.*, 1992; Schmidt *et al.*, 1993; 1994). L-NMMA competes with L-Arg, as well as L-lysine and L-ornithine, for the cationic amino acid system y^+ transporter, whereas inhibitors such as NOARG and L-NAME, compete with L-leucine and L-isoleucine for the neutral amino acid transporter, system L. Co-incubation of placental sections with amino acids selective for either the system y^+ or system L transporter had no apparent effect on [^{3}H]-L-NOARG binding, suggesting that the radiolabelled inhibitor was not competing for an amino acid transport system but for the L-Arg recognition site of eNOS.

Studies on isolated perfused placental cotyledons, in which NOS inhibitors were added to the foetoplacental circulation, have indicated that NO has a role in maintaining placental blood flow (Gude *et al.*, 1990; 1992; Myatt *et al.*, 1991; 1992). However, the addition of NO to the intervillous space, rather than the foetoplacental circulation itself, has been found to have no effect on perfusion pressure (Eis *et al.*, 1995), suggesting that trophoblast-derived NO may not have a significant influence on the tone of foetoplacental blood vessels. It is disputed whether or not there is intervillous blood flow in the first trimester (Jauniaux *et al.*, 1995), when high levels of NOS and enzyme activity were demonstrated in the villous trophoblast, but trophoblast-derived NO may have a role at the foeto-maternal interface, modulating platelet and leucocyte adhesion and aggregation (Myatt *et al.*, 1993a; Buttery *et al.*, 1994b; Eis *et al.*, 1995). In normal pregnancies, the spiral arteries supplying the villous space undergo structural changes as a result of trophoblast invasion, but in PE pregnancies this process is less extensive (Meekins *et al.*, 1994) and it is postulated that this results in reduced placental perfusion and endothelial cell dysfunction, as indicated by increased maternal pressor activity, reduced prostacyclin and NO release, increased thromboxane production and platelet activation (Roberts & Redman, 1993; McCarthy *et al.*, 1993; Seligman *et al.*, 1994). The apparent increase in trophoblast NOS and enzyme activity found in placentae from PE and IUGR complicated pregnancies may represent a compensatory response to these changes. Alternatively, differences in the maternal plasma concentration of the endogenous NOS inhibitor ADMA may influence trophoblast NOS expression, higher circulating levels having been found in PE women compared to normotensive controls (Fickling *et al.*, 1993). No correlation was found between gestational age and placental [^{3}H]-L-NOARG binding density in PE and IUGR pregnancies, however, the possibility cannot be excluded that the raised levels of NOS and enzyme activity found in these tissues also reflects differences in gestational age as women with pregnancies complicated by these conditions were delivered at an earlier gestational age compared to the normal-term controls. Previous studies have indicated that NO production by umbilical artery endothelium, as well as the sensitivity of the vessel to NO, also declines during pregnancy (Izumi *et al.*, 1994). The present findings demonstrate that villous trophoblast NOS levels and activity decline in normal pregnancy, between the first trimester and term. During the first trimester, placental trophoblast cells are highly proliferative, and as in cultured endothelial cells (Arnal *et al.*, 1994), this may be associated with increased NOS expression. Whether the trophoblast-derived NO has a role in the remodelling of the spiral arteries or acts as a local autocrine or paracrine factor modulating trophoblast cell growth and function remains to be determined.

The main stimulus to NO release in the foetoplacental vascular bed is more likely to be local blood flow and shear stress than receptor mediated mechanisms (Myatt *et al.*, 1992; Hull *et al.*, 1994), no significant receptor-mediated NO release having been detected *in vitro* from branches of stem villous vessels, denuded of trophoblast (McCarthy *et al.*, 1994). The relationship between increased vascular resistance in the foetoplacental circulation and the depletion of eNOS binding in the umbilical artery from PE and IUGR complicated pregnancies is not fully understood, but the latter could contribute to the impaired NO release described in the umbilical artery of PE women (Pinto *et al.*, 1991; Akar *et al.*, 1994). The decline in NO production found in the umbilical artery during normal pregnancy (Izumi *et al.*, 1994) suggests that the apparent depletion of eNOS binding in PE and IUGR complicated pregnancies was not due to the earlier delivery of these pregnancies compared to controls.

In conclusion, the radiolabelled NOS inhibitor [^{3}H]-L-NOARG appears to bind specifically to the endothelial isoform of the enzyme, this being localized to the placental villous trophoblast and vascular endothelium. NOS expression and activity varies in normal, PE and IUGR pregnancies. The role of trophoblast-derived NO in the control of human placental function remains to be elucidated, but the high levels of NOS demonstrated in the first trimester suggest a role for NO in the developing placenta. The elevated levels of NOS in placentae from pregnancies complicated by PE and IUGR, compared to normal-term controls, may represent a compensatory response to changes in the maternal circulation. Conversely, the apparent reduction in umbilical artery endothelial NOS expression in PE and IUGR complicated pregnancies may reflect the endothelial dysfunction which is a feature of these conditions.

This work was supported in part by the Medical Research Council. The authors would like to thank Patricia Harley for excellent technical assistance, Dr T.J. Evans for providing tissues from LPS-treated rats and Dr J.S. Pollock for the monoclonal antibody against bovine aortic eNOS.

References

AKAR, F., ARK, M., UYDES, B.S., SOYSAL, M.E., SARACOGLU, F., ABACIOGLU, N., VAN DE VOORDE, J. & KANZIK, I. (1994). Nitric oxide production by human umbilical vessels in severe pre-eclampsia. *J. Hypertension*, **12**, 1235–1241.

ARNAL, J-F., YAMIN, J., DOCKERY, S. & HARRISON, D.G. (1994). Regulation of endothelial nitric oxide synthase mRNA, protein, and activity during cell growth. *Am. J. Physiol.*, **267**, C1381–C1388.

BOGLE, R.G., MONCADA, S., PEARSON, J.D. & MANN, G.E. (1992). Identification of inhibitors of nitric oxide synthase that do not interact with the endothelial cell L-arginine transporter. *Br. J. Pharmacol.*, **105**, 768–770.

BOURA, A.L.A., WALTERS, W.A.W., READ, M.A. & LEITCH, I.M. (1994). Autocoids and control of human placental blood flow. *Clin. Exp. Pharmacol. Physiol.*, **21**, 737–748.

BREDT, D.S., HWANG, P.M., GLATT, C.E., LOWENSTEIN, C., REED, R.R. & SNYDER, S.H. (1991). Cloned and expressed nitric oxide synthase structurally resembles cytochrome P450 reductase. *Nature*, **351**, 714–718.

BREDT, D.S. & SNYDER, S.H. (1990). Isolation of nitric oxide synthetase, a calmodulin-requiring enzyme. *Biochemistry*, **87**, 682–685.

BRENNECKE, S.P., GUDE, N.M., DILULIO, J.L. & KING, R.G. (1994). Nitric oxide synthase activity in human placental villous tissue is reduced in pre-eclampsia. *Hypertens. Pregnancy*, **13**, 306.

BUSSE, R. & MULSCH, A. (1990a). Induction of nitric oxide synthase by cytokines in vascular smooth muscle cells. *FEBS. Lett.*, **275**, 87–90.

BUSSE, R. & MULSCH, A. (1990b). Calcium-dependent nitric oxide synthesis in endothelial cytosol is mediated by calmodulin. *FEBS Lett.*, **265**, 133–136.

BUTTERY, L.D.K., EVANS, T.J., SPRINGALL, D.R., CARPENTER, A., COHEN, J. & POLAK, J.M. (1994a). Immunochemical localization of inducible nitric oxide synthase in endotoxin-treated rats. *Lab. Invest.*, **71**, 755–764.

BUTTERY, L.D.K., MCCARTHY, A., SPRINGALL, D.R., SULLIVAN, M.H.F., ELDER, M.G. & POLAK, J.M. (1994b). Endothelial nitric oxide synthase in the human placenta: regional distribution and proposed regulatory role at the feto-maternal interface. *Placenta*, **15**, 257–265.

CHAUDHURI, G., BUGA, G.M., GOLD, M.E., WOOD, K.S. & IGNARRO, L.J. (1991). Characterization of actions of human umbilical endothelium derived relaxing factor. *Br. J. Pharmacol.*, **102**, 331–336.

CHENG, Y.C. & PRUSOFF, W.H. (1973). Relationship between the inhibition constant (K_i) and the concentration of inhibitor which causes 50 per cent inhibition (I_{50}) of an enzyme reaction. *Biochem. Pharmacol.*, **22**, 3099–3108.

CHO, H.J., XIE, Q-W, CALAYCAY, J., MUMFORD, R.A., SWIDEREK, K.M., LEE, T.D. & NATHAN, C. (1992). Calmodulin is a tightly bound subunit of calcium-calmodulin-independent nitric oxide synthase. *J. Exp. Med.*, **176**, 599–604.

CONRAD, K.P., JOFFE, G.M., KRUSZNYA, H., KRUSZNYA, R., ROCHELLE, L.G., SMITH, R.P., CHAVEZ, J.E. & MOSHER, M.D. (1993a). Identification of increased nitric oxide biosynthesis during pregnancy in rats. *FASEB J.*, **7**, 566–571.

CONRAD, K.P., VILL, M., MCGURIE, P.G., DAIL, W.G. & DAVIS, A.K. (1993b). Expression of nitric oxide synthase by syncytiotrophoblast in human placental villi. *FASEB J.*, **7**, 1269–1276.

EIS, A.L.W., BROCKMAN, D.E., POLLOCK, J.S. & MYATT, L. (1995). Immunohistochemical localization of endothelial nitric oxide synthase in human villous and extravillous trophoblast populations and expression during syncytiotrophoblast formation in vitro. *Placenta*, **16**, 113–126.

ERSKINE, R.L.A. & RITCHIE, J.W.L. (1985). Umbilical artery blood flow characteristics in normal and growth retarded fetuses. *Br. J. Obstet. Gynaecol.*, **92**, 605–610.

FICKLING, S.A., WILLIAMS, D., VALLANCE, P., NUSSEY, S.S. & WHITLEY, G.ST.J. (1993). Plasma concentrations of endogenous inhibitor of nitric oxide synthesis in normal pregnancy and pre-eclampsia. *Lancet*, **342**, 242–243.

FOX, S.B. & KHONG, T.Y. (1990). Lack of innervation of human umbilical cord. An immunohistological and histochemical study. *Placenta*, **11**, 59–62.

FURFINE, E.S., HARMON, M.F., PAITH, J.E. & GARVEY, E.P. (1993). Selective inhibition of constitutive nitric oxide synthase by L-N^G-nitroarginine. *Biochemistry*, **32**, 8512–8517.

GARVEY, E.D., TUTTLE, J.V., COVINGTON, K., MERRILL, B.M., WOOD, E.R., BAYLIS, S.A. & CHARLES, I.G. (1994). Purification and characterization of the constitutive nitric oxide synthase from human placenta. *Arch. Biochem. Biophys.*, **311**, 235–241.

GOETZ, R.M., MORANO, I., CALOVINI, T., STUDER, R. & HOLTZ, J. (1994). Increased expression of endothelial constitutive nitric oxide synthase in rat aorta during pregnancy. *Biochem. Biophys. Res. Commun.*, **205**, 905–910.

GUDE, N.M., BOURA, A.L.A., KING, R.G., BRENNECKE, S.P., JAMAL, O.S., SMITH, R. & WALTERS, W.A.W. (1992). Evidence for inhibition by endothelium-derived relaxing factor of thromboxane A_2 receptor-mediated vasoconstriction in fetal vessels of the human perfused placenta. *Placenta*, **13**, 597–605.

GUDE, N.M., KING, R.G. & BRENNECKE, S.P. (1990). Role of endothelium-derived nitric oxide in maintenance of low fetal vascular resistance in placenta. *Lancet*, **336**, 1589–1590.

HASAN, K., HEESEN, B-J., CORBETT, J.A., MCDANIEL, M.L., CHANG, K., ALLISON, W., WOLFFENBUTTEL, B.H.R., WILLIAMSON, J.R. & TILTON, R.G. (1993). Inhibition of nitric oxide formation by guanidines. *Eur. J. Pharmacol.*, **249**, 101–106.

HULL, A.D., WHITE, C.R. & PEARCE, W.J. (1994). Endothelium-derived relaxing factor and cyclic GMP-dependent vasorelaxation in human chorionic plate arteries. *Placenta*, **15**, 365–375.

IZUMI, H., GARFIELD, R.E., MAKINO, Y., SHIRAKAWA, K. & ITOH, T. (1994). Gestational changes in endothelium-dependent vasorelaxation in human umbilical artery. *Am. J. Obstet. Gynecol.*, **170**, 236–245.

JAUNIAUX, E., JURKOVIC, D. & CAMPBELL, S. (1995). In vivo investigation of the placental circulations by doppler echography. *Placenta*, **16**, 323–331.

KIDD, E.J., MICHEL, A.D. & HUMPHREY, P.P.A. (1995). Autoradiographic distribution of [^{3}H]-N^G-nitro-arginine binding in rat brain. *Neuropharmacol.*, **34**, 63–73.

KNOWLES, R.G. & MONCADA, S. (1994). Nitric oxide synthases in mammals. *Biochem. J.*, **298**, 249–258.

KOVÁCS, G.A., MAKARY, A., PETŐ, J. & STEINMETZ, G. (1994). Deficiency of c-GMP level in placental circulation in pregnancy-induced hypertensive disorders: possibility of decreased endothelium-derived relaxing factor activity. *Hyperten. Preg.*, **13**, 163–169.

LAEMMLI, U.K. (1970). Cleavage of structural proteins during the assembly of the head of Bacteriophage T4. *Nature.*, **227**, 680–685.

MARSDEN, P.A., SCHAPPERT, K.T., CHEN, H.S., FLOWERS, M., SUNDELL, C.L., WILCOX, J.N., LAMAS, S. & MICHEL, T. (1992). Molecular cloning and characterization of human endothelial nitric oxide synthase. *FEBS Lett.*, **307**, 287–293.

MCCARTHY, A.L., WOOLFSON, R.G., EVANS, B.J., DAVIES, D.R., RAJU, S.K. & POSTON, L. (1994). Functional characteristics of small placental arteries. *Am. J. Obstet. Gynecol.*, **170**, 945–951.

MCCARTHY, A.L., WOOLFSON, R.G., RAJU, S.K. & POSTON, L. (1993). Abnormal endothelial function of resistance arteries from women with preeclampsia. *Am. J. Obstet. Gynecol.*, **168**, 1323–1330.

MEEKINS, J.W., PIJNENBORG, R., HANSSENS, M., MCFADYEN, I.R. & VAN ASSHE, A. (1994). A study of placental bed spiral arteries and trophoblast invastion in normal and severe pre-eclamptic. *Br. J. Obstet. Gynaecol.*, **101**, 669–674.

MICHEL, A.M., PHUL, R.K., STEWART, T.L. & HUMPHREY, P.P.A. (1993). Characterization of the binding of [^{3}H]-L-N^G-nitro-arginine in rat brain. *Br. J. Pharmacol.*, **109**, 287–288.

MISKO, T.P., MOORE, W.M., KASTEN, T.P., NICKOLS, G.A., CORBETT, J.A., TILTON, R.G., MCDANIEL, M.L., WILLIAMSON, J.R. & CURRIE, M.G. (1993). Selective inhibition of the inducible nitric oxide synthase by aminoguanidine. *Eur. J. Pharmacol.*, **233**, 119–125.

MOLNÁR, M. & HERTELENDY, F. (1992). N^G-nitro-L-arginine, an inhibitor of nitric oxide synthesis, raises blood pressure in rats and reverses the pregnancy-induced refractoriness to vassopressor agents. *Am. J. Obstet. Gynecol.*, **166**, 1560–1567.

MOLNÁR, M., SÜTŐ, T., TÓTH, T. & HERTELENDY, F. (1994). Prolonged blockade of nitric oxide synthesis in gravid rats produces sustained hypertension, proteinuria, thrombocytopenia and intrauterine growth retardation. *Am. J. Obstet. Gynecol.*, **170**, 1458–1466.

MYATT, L., BREWER, A. & BROCKMAN, D.E. (1991). The action of nitric oxide in the perfused human fetal-placental circulation. *Am. J. Obstet. Gynecol.*, **164**, 687–692.

MYATT, L., BREWER, A., LANGDON, G. & BROCKMAN, D.E. (1992). Attenuation of the vasoconstrictor effects of thromboxane and endothelin by nitric oxide in the human fetal-placental circulation. *Am. J. Obstet. Gynecol.*, **166**, 224–230.

MYATT, L., BROCKMAN, D.E., EIS, A.L.W. & POLLOCK, J.S. (1993a). Immunohistochemical localization of nitric oxide synthase in the human placenta. *Placenta*, **14**, 487–495.

MYATT, L., BROCKMAN, D.E., LANGDON, G. & POLLOCK, J.S., (1993b). Constitutive calcium-dependent isoform of nitric oxide synthase in the human placental villous vascular tree. *Placenta*, **14**, 373–383.

PINTO, A., SORRENTINO, R., SORRENTINO, P., GUERRITORE, T., MIRANDA, L., BIONDI, A. & MARTINELLI, P. (1991). Endothelial-derived relaxing factor released by endothelial cells of human umbilical vessels and its impairment in pregnancy-induced hypertension. *Am. J. Obstet. Gynecol.*, **164**, 507–513.

POLLOCK, J.S., FORSTERMANN, U., MITCHELL, J.A., WARNER, T.D., SCHMIDT, H.H.H.W., NAKANE, M. & MURAD, F. (1991). Purification and characterization of particulate endothelium-derived relaxing factor synthase from cultured and native bovine aortic endothelial cells. *Proc. Natl. Acad. Sci. U.S.A.*, **309**, 402–404.

POLLOCK, J.S., NAKANE, M., BUTTERY, L.D.K., MARTINEZ, A., SPRINGALL, D.R., POLAK, J.M., FORSTERMANN, U. & MURAD, F. (1993). Characterization and localization of endothelial nitric oxide synthase using specific monoclonal antibodies. *Am. J. Physiol.*, **34**, C1379–C1387.

REILLY, F.D. & RUSSELL, P.T. (1977). Neurohistochemical evidence supporting an absence of adrenergic and cholinergic innervation in the human placenta and umbilical cord. *Anat. Rec.*, **188**, 277–286.

ROBERTS, J.M. & REDMAN, C.W.G. (1993). Pre-eclampsia: more than pregnancy-induced hypertension. *Lancet*, **341**, 1447–1454.

SCHMIDT, K., KLATT, P. & MAYER, B. (1993). Characterization of endothelial cell amino acid transport systems involved in the actions of nitric oxide synthase inhibitors. *Molec. Pharmacol.*, **44**, 615–621.

SCHMIDT, K., KLATT, P. & MAYER, B. (1994). Uptake of nitric oxide synthase inhibitors by macrophage RAW 264.7 cells. *Biochem. J.*, **301**, 313–316.

SELIGMAN, S.P., BUYON, J.P., CLANCY, R.M., YOUNG, B.K. & ABRAMSON, S.B. (1994). The role of nitric oxide in the pathogenesis of preeclampsia. *Am. J. Obstet. Gynecol.*, **171**, 944–948.

SESSA, W.C. (1994). The nitric oxide family of proteins. *J. Vasc. Res.*, **31**, 131–143.

SESSA, W.C., BARBER, C.M. & LYNCH, K.R. (1993). Mutation of N-myristoylation site converts endothelial cell nitric oxide synthase from a membrane to a cytosolic protein. *Circ. Res.*, **72**, 1–4.

SPRINGALL, D.R., RIVEROS-MORENO, V., BUTTERY, L., SUBURO, A., BISHOP, A.E., MERRETT, M., MONCADA, S. & POLAK, J.M. (1992). Immunological detection of nitric oxide synthase(s) in human tissues using heterologous antibodies suggesting different isoforms. *Histochemistry*, **98**, 259–266.

STUEHR, D.J., CHO, H.J., KWON, N.S., WEISE, M. & NATHAN, C.F. (1991). Purification and characterisation of the cytokine-induced macrophage nitric oxide synthase: an FAD- and FMN-containing flavoprotein. *Proc. Natl. Acad. Sci. U.S.A.*, **88**, 7773–7777.

TRUDGINER, B.J., GILES, W.B., COOK, C.M., BONBARDIERI, J. & COLLINS, L. (1985). Fetal umbilical waveforms and placental resistance: clinical significance. *Br. J. Obstet. Gynaecol.*, **92**, 23–30.

WALLENSTEIN, S., ZUCKER, C.L. & FLEISS, J.L. (1980). Some statistical methods useful in circulation research. *Circ. Res.*, **47**, 1–9.

WANG, Y., WALSH, S.W., PARNELL, R. & HAN, J. (1994). Placental production of nitric oxide and endothelin in normal and preeclamptic pregnancies. *Hypertens. Preg.*, **13**, 171–178.

WHITE, M. (1985). The transport of cationic amino acids across the plasma membrane of mammalian cells. *Biochim. Biophys. Acta*, **822**, 355–374.

XIE, Q., CHO, H.J., CALAYCAY, J., MUMFORD, R.A., SWIDEREK, K.M., LEE, T.D., DING, A., TROSO, T. & NATHAN, C. (1992). Cloning and characterization of inducible nitric oxide synthase from mouse macrophages. *Science*, **256**, 225–228.

YALLAMPALLI, C. & GARFIELD, R.E. (1993). Inhibition of nitric oxide synthesis in rats during pregnancy produces signs similar to those of preeclampsia. *Am. J. Obstet. Gynecol.*, **169**, 1316–1320.

(Received July 5, 1995
Revised August 8, 1995
Accepted September 4, 1995)